Thermodynamic Dissection of the Substrate−Ribozyme Interaction in the Hammerhead Ribozyme†

Klemens J. Hertel,‡ Tracy K. Stage-Zimmermann,§ Glenyss Ammons, and Olke C. Uhlenbeck*

Department of Chemistry and Biochemistry, University of Colorado, Boulder, Colorado 80309-0215

Received July 20, 1998; Revised Manuscript Received September 21, 1998

ABSTRACT: The free energy of substrate binding to the hammerhead ribozyme was compared for 10 different hammerheads that differed in the length and sequence of their substrate recognition helices. These hammerheads were selected because neither ribozyme nor substrate oligonucleotide formed detectable alternate secondary structures. The observed free energies of binding varied from −8 to −24 kcal/mol and agreed very well with binding energies calculated from the nearest-neighbor free energies if a constant energetic penalty of $\Delta G^\circ_{core} = +3.3 \pm 1$ kcal/mol is used for the catalytic core. A set of substrates that contained a competing hairpin secondary structure showed weaker binding to the ribozyme by an amount consistent with the predicted free energy for hairpin formation. These thermodynamic conclusions permit the prediction of substrate binding affinities for ribozyme−substrate pairs of any helix length and sequence, and thus, should be very valuable for the rational design of ribozymes directed toward gene inactivation.

In the bimolecular format used for mRNA cleavage experiments, the hammerhead consists of a ribozyme oligonucleotide of 35−45 nucleotides and a 12−20 nucleotide substrate sequence that is embedded within a target mRNA (*1*). The ribozyme binds its substrate through the formation of two RNA helices termed helix I and helix III (Figure 1A). After substrate binding, cleavage occurs at a unique site and the two product RNAs subsequently dissociate. While numerous successful applications of mRNA cleavage by hammerhead ribozymes inside cells have been reported, there are also many examples where hammerheads were not effective at cleaving RNA targets either in vivo or in vitro (reviewed in refs *2*−*5*). A careful kinetic and thermodynamic analysis of the hammerhead cleavage reaction should help to understand the reasons for these disparate observations.

This study focuses on the energetics of substrate binding to the ribozyme. The formation of the two RNA stems is expected to stabilize substrate binding in a manner that depends on the length and sequence of the helices. However, substrate binding also causes the conserved catalytic core of the hammerhead to assemble, resulting in the formation of a noncanonical base pair ($A_{15.1}$−$U_{16.1}$) and several hydrogen bonds involving 2′ hydroxyls (*6, 7*). The energetic contribution of these core interactions to substrate binding affinity is unknown; however, it is expected to be similar for all hammerheads. Previous studies of several ribozyme−substrate pairs found that ribozymes with long helices bound their substrates more tightly than those with short helices (*8, 9*). This led to the suggestion that the free energy of substrate binding could be described by a constant core contribution and a variable helical contribution that depended upon the length and sequence of the helices (*8*). However, certain other hammerheads showed unusually weak substrate binding, which was attributed to the formation of alternate conformations or aggregates of the ribozyme and/or substrate oligonucleotides (*9*). This paper attempts to confirm the original suggestion by examining the substrate binding affinities of a number of hammerheads that have different helix lengths and sequences and that do not form detectable alternate structures. The measured free energies for substrate binding are compared to the free energy of an uninterrupted RNA helix calculated from the well-established rules for RNA helix formation (*10*). In addition, the binding of a ribozyme to a series of substrates having competing hairpin secondary structures is determined in order to explore the energetic consequences of reduced substrate accessibility.

MATERIALS AND METHODS

RNA Synthesis. All ribozyme oligonucleotides were synthesized by in vitro transcription with T7 RNA polymerase using synthetic DNA templates and purified by gel electrophoresis (*9, 11*). All substrate oligonucleotides were chemically synthesized, deprotected, gel-purified, and [5′-^{32}P]-labeled as previously described (*12*). RNA concentrations were calculated by assuming a residue extinction coefficient $E_{260} = 8500\ M^{-1}\ cm^{-1}$.

Hammerhead Kinetics and Thermodynamics. All reactions were performed at 25 °C in a buffer containing 10 mM $MgCl_2$ and 50 mM Tris-HCl or K-Hepes buffer at pH 7.5 unless otherwise indicated. k_{cat} and K_d values were determined by varying the ribozyme concentration with trace labeled substrate as previously described (*13*), by the protocol that uses the addition of $MgCl_2$ to start the reaction (*8*). Dilution chase experiments to evaluate k_{-1} were performed

† This work was supported by NIH Grants GM 36944 and AI 30242.

* To whom correspondence should be addressed.

‡ Present address: Department of Molecular and Cellular Biology, Harvard University, 7 Divinity Ave., Cambridge, MA 02113.

§ Present address: Department of Biological Chemistry and Molecular Pharmacology, Harvard Medical School, and Department of Cancer Biology, Dana Farber Cancer Institute, 44 Binney St., Boston, MA 02115.

10.1021/bi981740b CCC: $15.00
Published on Web 11/10/1998

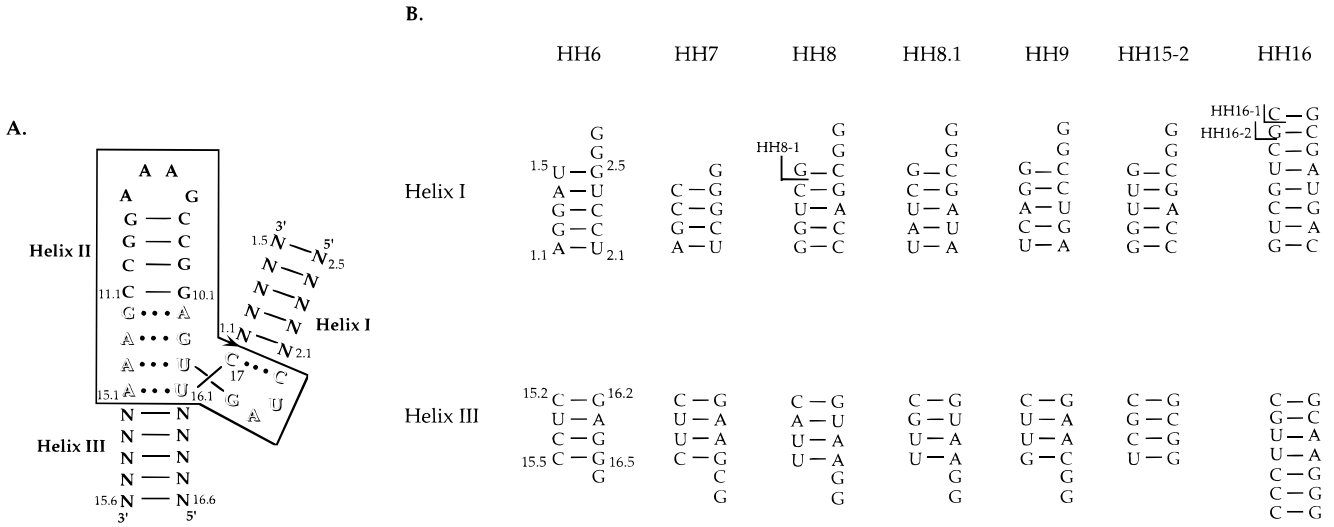

FIGURE 1: (A) Secondary structure of the hammerhead depicted to reflect the crystal structure and in the format used for mRNA cleavage experiments. The constant region is enclosed by the box consisting of helix−loop II and the conserved core nucleotides. Helices I and III can be of any sequence and length (N = A, U, C, or G). The numbers indicate nucleotide positions according to standard nomenclature (*30*). (B) Helix I and III sequences of the hammerhead ribozymes: HH8−1 and HH16−1 are derivatives of HH8 and HH16 where the 3′ terminal nucleotide of the substrate is removed. HH16−2 deletes two nucleotides.

as previously described (*13*, *14*). To determine the second-order rate constant (k_{cat}/K_M) for S8D and S8E, the rate of cleavage was observed at 1, 3, 5, or 15 μM ribozyme 8, <0.2 nM S8D or S8E, K−Hepes, pH 7.5, 10 mM $MgCl_2$, and 25 °C. Ribozyme and substrate oligonucleotides were mixed in Hepes buffer and heated to 95 °C for 1.5 min to disrupt aggregates. After cooling to 25 °C, the reaction was initiated by adding magnesium. The reaction rates increased with increasing ribozyme concentration as expected and k_{cat}/K_M was calculated from the relationship $k_{obs} = (k_{cat}/K_M)[R]$. K_d values were converted to free energies of substrate binding by the relationship $\Delta G°_{E\cdot S} = RT \ln K_d$.

Nondenaturing gels were used to evaluate the extent that substrates S8A−S8E formed dimers as a function of concentration. [5′-^{32}P]-Labeled oligonucleotide was mixed with nonradioactive oligonucleotide in 50 mM Tris-HCl, pH 7.5, to give final concentrations from 5 nM to 0.015 nM in a volume of 9 μL. The RNAs were heated at 95 °C for 1.5 min and cooled to 25 °C prior to the addition of 1 μL of 0.1 M $MgCl_2$. After incubation at 25 °C for 15−25 min, 2 μL of 30% glycerol and dyes was added to each sample. Reactions were loaded on a 15% acrylamide/50 mM Tris−acetate, pH 7.5/10 mM $MgCl_2$ gel at 25 °C and run overnight in the cold room. The fraction dimer at each substrate concentration was quantitated by a Molecular Dynamics Phosphorimager.

RESULTS

Determination of K_d Values. The sequences of stem−loop II and domain I and II are identical for all hammerheads described in this work and most of those described elsewhere. Therefore, this region will be referred to as the core. The nucleotide at the cleavage site (position 17) for all substrates tested was cytosine. However, this position can be varied and those effects on substrate binding are described elsewhere (*15*). The sequences of helices I and III for the 10 different hammerheads studied in this work are shown in Figure 1B. Their helix lengths varied from 8 to 16 base pairs, which covered the range typically used for mRNA cleavage experiments. All 10 of these hammerheads were chosen because neither the ribozyme nor the substrate oligonucleotides showed evidence for alternate structures on the basis of two independent criteria. First, analysis of each oligonucleotide on nondenaturing gels gave a single band between 0.2 nM and 1 μM oligonucleotide. Second, kinetic progress curves with saturating ribozyme and trace labeled substrate went to near completion (>90%) and fit a first-order rate equation.

Because our interest focused on the affinity of the ribozyme for the substrate, all experiments were performed with a large excess of ribozyme over the substrate so that only the binding and cleavage and not the product release steps of the reaction were considered. Thus, a simple two-step reaction pathway describes the mechanism of hammerhead cleavage (Scheme 1).

Scheme 1

$$E + S \underset{k_{-1}}{\overset{k_1}{\rightleftharpoons}} E\cdot S \underset{k_{-2}}{\overset{k_2}{\rightleftharpoons}} E\cdot P1\cdot P2$$

Despite this simplification, the method for determination of $K_d = k_{-1}/k_1$ depends on the kinetic properties of the individual ribozyme tested. If k_{-1} is much faster than k_2, K_d can be obtained by measuring the rate of cleavage as a function of ribozyme concentration (*13*, *16*). If k_{-1} is not faster than k_2, another method for determining K_d must be used. To evaluate the difference between k_{-1} and k_2 for each hammerhead, a dilution partitioning experiment was used (*14*). Because k_{-1} for HH7, HH8, HH8−1, HH8.1, HH9, and HH15−2 were found to be fast compared to k_2, K_d could be determined from the ribozyme saturation experiment (Table 1). For HH6, k_{-1} was measured directly from the partitioning experiment to be 0.6 min^{-1}. The K_d value was then calculated from the experimentally determined K_M of 46 nM and $K_M = (k_2 + k_{-1})/k_1$. For HH16, HH16−1, and HH16−2, K_d was calculated indirectly from the internal equilibrium, the product binding equilibria, and the overall reaction equilibrium (*8*). As shown in Table 1, the K_d values

Table 1: Cleavage Properties of Hammerheads[a]

hammerhead	k_2 (min^{-1})	K_d (nM)	$\Delta G°_{E·S}$(expt) (kcal/mol)	$\Delta G°_{helix}$ (kcal/mol)
HH6	1.5	13	−10.8	−13.5
HH7	0.4	400	−8.7	−11.6
HH8[b]	1.3	41	−10.0	−12.3
HH8−1	1.4	2700	−7.6	−10.4
HH8.1	0.4	5000	−7.2	−9.1
HH9[b]	1.5	160	−9.2	−12.2
HH15−2	1.0	700	−8.4	−12.4
HH16[c]	1.0	4×10^{-9}	−23.8	−28.3
HH16−1[d]	1.0	5.3×10^{-5}	−19.4	−23.8
HH16−2[d]	0.7	2.6×10^{-4}	−17.1	-21.7

[a] All experiments were performed at 10 mM $MgCl_2$ and 50 mM Hepes or Pipes buffer, pH 7.5 at 25 °C, except for HH8.1, which was measured at pH 6.5. $\Delta G°_{E·S} = RT \ln K_d$. $\Delta G°_{helix}$ was obtained from the free energy values in Freier et al. (*10*). [b] Data from Fedor and Uhlenbeck, (*9*). [c] Data from Hertel et al. (*8*). [d] Data from Hertel et al. (*29*).

for the 10 hammerheads vary over a range of 10^{12}, spanning nearly the entire range that is experimentally accessible. Weaker K_d values would require inconveniently high concentrations of oligonucleotides, and tighter K_d values would involve product helices so long that their affinities could not be accurately determined by native gel methods.

Correlation of Measured K_ds to Predicted Values. The free energy of substrate binding for each hammerhead can also be estimated by using the thermodynamic principles for RNA folding summarized by Turner and co-workers (*10*, *17*, *18*). In this case, the free energy of substrate binding[1] is equal to the sum of the favorable contribution of helix I and helix III ($\Delta G°_{helix}$) and the contribution of the catalytic core ($\Delta G°_{core}$) according to eq 1. $\Delta G°_{helix}$ was calculated from the sum of a single bimolecular initiation penalty ($\Delta G°_{i} = +3.2$ kcal/mol), the free energies for helix I and helix III of each hammerhead ($\Delta G°_{NN}$) calculated from the empirically determined free energies for base pairing, and the free energy contribution for any 3′ or 5′ dangling nucleotides ($\Delta G°_{dangle}$) according to eq 2.

$$\Delta G°_{E·S}(\text{calc}) = \Delta G°_{core} + \Delta G°_{helix} \quad (1)$$

$$\Delta G°_{helix} = \Delta G°_{i} + \Delta G°_{NN} + \Delta G°_{dangle} \quad (2)$$

The calculated values of $\Delta G°_{helix}$ for the 10 hammerheads are summarized in Table 1 and are graphically compared to the experimental values [$\Delta G°_{E·S}$(expt)] in Figure 2. Very good correlation is observed, giving a slope close to 1 and a *y*-intercept of 3.1 kcal/mol. The slope of 1 clearly supports the idea that changes in hammerhead substrate affinity are due to differences in the free energy of helix formation. The *y*-intercept is the free energy penalty of interrupting the semicontinuous I−III helix with the core nucleotides, $\Delta G°_{core} = 3.1$ kcal/mol. The *y*-intercept value of $\Delta G°_{core} = 3.1$ kcal/mol is in very good agreement with the average value of $\Delta G°_{core} = 3.3 \pm 1$ kcal/mol derived from the individual $\Delta G°_{core}$ values (Table 1).

The excellent correlation between the experimental and calculated values of hammerhead substrate binding energies shown in Figure 2 suggests that substrate binding energies

[1] All free energies discussed in this paper are at 25 °C unless mentioned.

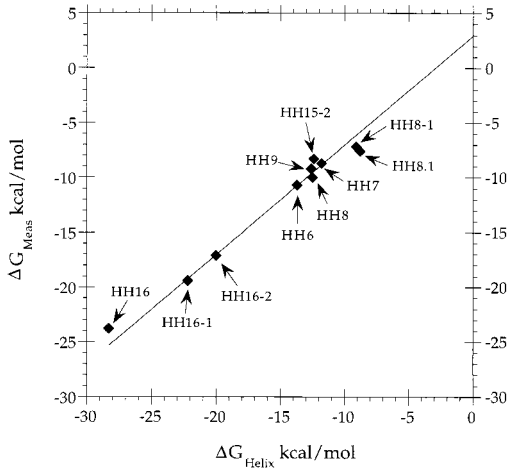

FIGURE 2: Correlation between the measured free energy of substrate binding $\Delta G°_{E·S}$(expt) and the free energy of RNA helix formation ($\Delta G°_{helix}$). The line has a slope of 1 and an intercept of +3.1 kcal/mol, which is equal to $\Delta G°_{core}$.

for hammerheads with any helix length or sequence can be predicted from the calculated $\Delta G°_{helix}$ and a value for $\Delta G°_{core}$ of $+3.3 \pm 1$ kcal/mol. Because all of the hammerheads used to establish this correlation (Figure 2) are kinetically well behaved, the prediction of $\Delta G°_{E·S}$ values for new hammerheads are based on the assumption that they do not form alternate structures. If either the ribozyme or substrate oligonucleotides for a new hammerhead have alternate structures, the experimental $\Delta G°_{E·S}$ will be less favorable (more positive) than that predicted from Figure 2.

Effects of Substrate Structure on Cleavage Efficiency. To test whether the presence of alternate structures can lead to such a difference between the calculated and experimental values of $\Delta G°_{E·S}$, the cleavage properties of a series of five substrates for ribozyme 8 were examined. Each substrate was extended at its 5′ end such that an RNA hairpin could form and therefore interfere with binding to the ribozyme (Figure 3). The calculated free energy of formation for each of the hairpins indicated that the S8A and S8B hairpins were not likely to be stable at 25 °C and that S8C, S8D, and S8E formed increasingly stable secondary structures (Table 2). Although these oligonucleotides could also potentially form dimers (or larger aggregates), analysis on nondenaturing gels indicated that at concentrations of 1 nM for S8C and 0.2 nM for S8D and S8E, only monomers were detected (data not shown). The binding affinities of the five substrates to the ribozyme oligonucleotide were therefore determined with radiolabeled substrate below the dimerization concentration. Because k_{-1} is faster than k_2 for HH8, the substrate dissociation constants for the hairpin substrates are also expected to be faster than k_2. As shown in Table 2, the cleavage properties of S8A and S8B were found to be virtually identical to S8 at both saturating and subsaturating concentrations of ribozyme, consistent with the prediction that the corresponding hairpins do not form significantly at the reaction conditions.

In contrast to S8A and S8B, cleavage rates of S8C−S8E were greatly reduced at ribozyme concentrations sufficient to saturate the shorter substrates, suggesting that the formation of the hairpins impeded cleavage. In the case of S8C, complete cleavage of the substrate can be observed at longer incubation times and sufficiently high ribozyme concentra-

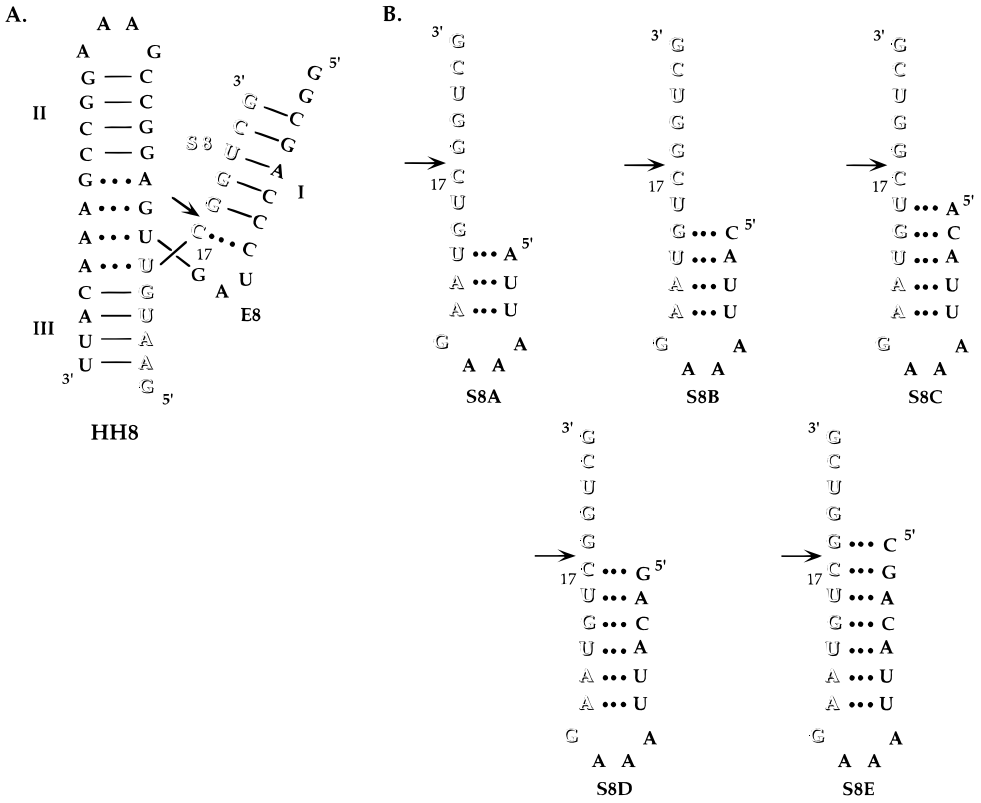

FIGURE 3: (A) Hammerhead 8 (HH8) with its unstructured substrate oligonucleotide in outlined type. (B) Five elongated versions of substrate 8 that contain potential intramolecular hairpin secondary structures. Outlined letters indicate the substrate 8 sequence.

Table 2: Effect of Substrate Structure on Cleavage Properties[a]

substrate	k_{cat} (min^{-1})	K_d (nM)	$\Delta G°_{E\cdot S}$(expt) (kcal/mol)	$\Delta G°_{hairpin}$ (kcal/mol)	$\Delta G°_{E\cdot S}$(calc) (kcal/mol)
S8	1.4	50[b]	−9.9		−9.9
S8A	1.2	38	−10.1	>0	−9.9
S8B	1.3	52	−9.9	>0	−9.9
S8C	0.4	2.4×10^3	−7.6	−1.5	−8.4
S8D	(0.4)	2×10^6 [c]	−3.7	−6.0	−3.9
S8E	(0.4)	4.6×10^7 [c]	−1.8	−7.7	−2.2

[a] Experiments were performed in 10 mM $MgCl_2$ and 50 mM Hepes buffer, pH 7.5 at 25 °C. $\Delta G°_{E\cdot S}(expt) = RT \ln K_d$. $\Delta G°_{hairpin}$ calculated from free energy rules (*10*) assuming $\Delta G°_{loop} = +5.5$ kcal/mol at 298 K. $\Delta G°_{E\cdot S}(calc) = -9.9$ kcal/mol $- \Delta G°_{hairpin}$. [b] Data from Fedor and Uhlenbeck (*13*). [c] Calculated from experimental second-order rate constant assuming $k_{cat} = 0.4$ min^{-1}.

tions. Reasonably accurate values of $k_{cat} = 0.4$ min^{-1} and $K_d = 2.4$ μM were obtained with a series of ribozyme concentrations up to 10 μM. Thus, the poor cleavage efficiency of S8C is primarily due to weaker substrate binding, presumably because of the competing hairpin secondary structure. In the case of S8D and S8E, cleavage rates were much slower but increased proportionally with increasing ribozyme concentration. Although high extents of cleavage of S8D could be observed at high ribozyme concentration and long incubation times, it was not possible to reach saturation for either substrate. At the highest ribozyme concentration tested (15 μM), the cleavage rates were 0.003 min^{-1} for S8D and 0.00013 min^{-1} for S8E, corresponding to apparent second-order rate constants of 2.0×10^2 M^{-1} min^{-1} and 8.7 M^{-1} min^{-1}, respectively. For the purposes of Table 2, the values of K_d were calculated from the measured second-order rate constants by assuming the same k_{cat} (0.4 min^{-1}) observed for S8C.

It is clear from the data in Table 2 that, as expected, the substrate binding affinity decreased dramatically as the stability of the hairpin increased. For example, increasing the stability of the hairpin by a single base pair between S8B and S8C increased the K_M approximately 50-fold from 52 nM to 2.4 μM. These measured affinities can be compared to a theoretical thermodynamic prediction by assuming that the equilibrium between an inactive hairpin substrate (H) and an active single-stranded substrate (S) is directly coupled to the ribozyme binding equilibrium (Scheme 2).

Scheme 2

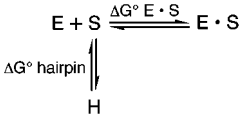

If this is the case, the free energy of substrate binding for a hairpin substrate can be estimated by subtracting the value of $\Delta G°_{hairpin}$ calculated from the free energy rules of hairpin formation (*10*) from the $\Delta G°_{E\cdot S}$ of S8. As shown in Table 2, the estimated values for binding of the hairpin substrates to the ribozyme [$\Delta G°_{E\cdot S}$(calc)] agree quite well with those determined experimentally.[2] Thus, it appears that a simple

[2] $\Delta G°_{hairpin}$ was calculated with a thermodynamic penalty of +5.5 kcal/mol for hairpin initiation at 25 °C, which is adjusted from 5.9 kcal/mol reported for a four-base hairpin loop at 37 °C (*10*). Initiation free energies for hairpins depend on loop sequence and can vary substantially. For example, if one uses a more recent average value for four base hairpin loops of +3.9 kcal/mol (*18*), the absolute agreement between experimental and calculated $\Delta G°_{E\cdot S}$ in Table 2 would be less accurate. However, the calculated incremental free energy differences between the substrates of varying length would continue to agree well with the experimental data.

thermodynamic competition model adequately explains the lower cleavage efficiency of the hairpin substrates.

DISCUSSION

The free energy of substrate binding by the hammerhead ribozyme correlates well with the values estimated from the formation of the two substrate binding arms calculated by the nearest-neighbor free energy rules. Although the correlation was expected (*8*), it was unclear how well the two data sets would agree quantitatively, considering the very different methods used to obtain the binding energies. In the case of the hammerhead, the data were derived from analysis of cleavage rate kinetics and from K_d measurements using nondenaturing gels. By contrast, the free energy rules were derived from absorbance−temperature profiles of many short RNA duplexes. It is important to note that, in both cases, data were only included if the oligonucleotides did not fold into alternate structures. Hammerheads that had detectable alternate conformations of the ribozyme or substrate were not used in this analysis. Similarly, helices that did not show all-or-none melting transitions were not considered for deducing the nearest-neighbor free energies. Figure 2 illustrates the excellent quantitative agreement between the two sets of energies. A linear plot with near-unitary slope is observed over a range of 20 kcal/mol. This correlation is especially remarkable considering that the two data sets were performed in different buffers. The hammerhead data was determined in low ionic strength and 10 mM Mg^{2+}, while the nearest-neighbor energies are determined at 1 M NaCl. This suggests that the electrostatic contribution to the free energy is negligible in both buffers and implies that there is no thermodynamically significant site for binding of Mg^{2+} to the two RNA helices. A contribution of site-specific Mg^{2+} to the free energy associated with stem−loop II and the core remains possible. Another example of close correlation between helix stabilities determined by a ribozyme assay in a Mg^{2+} buffer and calculated from the same nearest-neighbor free energies has been reported by Narlikar et al. (*19*) in their analysis of the formation of the substrate binding helix of the group I ribozyme.

A uniform unfavorable free energy of $+3.3 \pm 1$ kcal/mol can be assigned to the hammerhead core, which interrupts the substrate binding helices. This unfavorable free energy contributes to the stability of the hammerhead ribozyme−substrate complex. From the perspective of RNA structure prediction, the hammerhead core can be considered as a highly asymmetric 13 nucleotide internal loop. Estimates for the free energy of such a loop are greater than +6.1 kcal/mol at 37 °C (*10, 18*), a value much more unfavorable than the experimental value of ΔG°_{core} of $+3.3 \pm 1$ kcal/mol. Indeed, ΔG°_{core} more closely reflects the free energy of a single bulged nucleotide ($\Delta G^\circ_{37} = +3.9$ kcal/mol) or much smaller asymmetric internal loops ($\Delta G^\circ_{37} = +3.1-3.6$ kcal/mol) (*10*). Thus, the hammerhead core behaves thermodynamically as if it is a small internal loop, consistent with the observation that most of domain II of the catalytic core is already formed in the free ribozyme (*20*).

The results support the general view that hammerhead cleavage kinetics can be understood as a combination of the uniform cleavage and ligation properties of the catalytic core and the known kinetic properties of RNA helix formation and dissociation. The hammerhead kinetic scheme is defined in three phases, substrate binding to the ribozyme, the chemical cleavage−ligation step, and the product release steps (*13*). The data presented here show that the substrate binding equilibrium is dominated by the free energy for formation of helix I and helix III. Because the rate constant for substrate association (*8, 13*) is very similar to that measured for the formation of short RNA duplexes (*21*−*23*), differences in substrate binding affinity between various hammerhead sequences result from changes in the substrate dissociation rate constant. The cleavage−ligation step has been the subject of intense investigation in many laboratories. Although the cleavage rate is dependent on pH, temperature, and divalent metal ion concentration, it is not dependent upon the length or sequence of the helices (*9, 16, 24*). Finally, the product release steps, although not yet studied in great detail, appear to correlate closely with expected stabilities for RNA helix formation (*8, 13*). The equilibrium and rate constants associated with product release appear to be independent of the hammerhead core and can also be predicted by nearest-neighbor free energy rules. Thus, it is now possible to predict all of the elemental rate constants for the hammerhead ribozyme cleavage reaction with reasonable accuracy for any substrate recognition sequence, provided that the ribozyme or substrate does not form alternate structures.

The ability to predict the kinetic properties of any given hammerhead is valuable for the process of choosing efficient ribozymes for mRNA cleavage experiments. The value of $\Delta G^\circ_{E\cdot S}$ for a candidate ribozyme can be measured and compared to the calculated value. If the values are not in agreement, it is very likely that either the candidate ribozyme or substrate is forming an alternate structure that is weakening substrate binding and thereby reducing the efficacy of the ribozyme. The cleavage assay is a preferable alternative to native gel electrophoresis as a means to detect alternate conformations because native gels do not always resolve alternate conformations and often do not detect alternate structures that exchange rapidly with the native form. As reviewed recently (*16*), the problem of alternate ribozyme or substrate structures is frequently encountered when new ribozymes are tested.

When a ribozyme target sequence is embedded within a long RNA, the likelihood is high that it will participate in a secondary structure with some other part of the sequence, potentially reducing its accessibility to the ribozyme (*25, 26*). To analyze this situation, a series of substrates of the well-characterized hammerhead 8 were prepared that formed alternate hairpin secondary structures and as a result were predicted to reduce the ribozyme−substrate binding affinity. As expected, when the hairpin alternate structure was thermodynamically stable, substrate binding became weaker. In one case (S8C), it was possible to show that substrate binding was affected 50-fold by a single additional base pair while the catalytic step of the reaction was not significantly altered. This clearly illustrates how secondary structure within the target can dramatically affect cleavage.

A simple thermodynamic competition model was used to predict the substrate binding affinity of the hairpin substrates. For each substrate, the calculated free energy of hairpin formation was subtracted from the value of $\Delta G^\circ_{E\cdot S}$ for HH8

complexed to its unstructured substrate. As expected, a 2−3 kcal/mol incremental increase in $\Delta G^{\circ}_{E\cdot S}$(expt) was observed as the hairpin was elongated by single base pairs. The agreement between theoretical and experimental values thus strongly supports the single competition model and suggests that the affinity of the ribozyme binding to a substrate with known secondary structure can be predicted from nearest-neighbor free energy parameters.

It is likely that the thermodynamic and kinetic concepts developed here can be extended to mRNA cleavage by ribozymes inside prokaryotic and eukaryotic cells. While there is abundant evidence that mRNA forms defined secondary structures, it is unclear whether the established free energy rules for RNA folding are the same. Some evidence suggests, however, that the in vivo free energies are unlikely to be dramatically different from those measured in vitro. In an elegant application of a thermodynamic competition model, van Duin and co-workers showed that the efficiency of translational initiation of structured mRNAs in *Escherichia coli* could be accurately predicted from the free energy parameters determined in vitro (*27*, *28*). It is unknown whether a similar correlation would be observed in eukaryotic cells where the presence of many mRNA binding proteins may significantly affect the free energy values. An additional obstacle to understanding hammerhead kinetics in vivo is to determine the rate of the chemical step at intracellular conditions. For example, the much lower intracellular magnesium concentration is expected to reduce k_2 substantially. Once the rate of the chemical step is known, it will be interesting to perform experiments similar to those reported here, but inside cells.

REFERENCES

1. Haseloff, J., and Gerlach, W. L. (1988) *Nature 334*, 585−591.
2. Christoffersen, R. E., and Marr, J. J. (1995) *J. Med. Chem. 38*, 2023−2037.
3. Rossi, J. J. (1995) *Trends Biotechnol. 13*, 301−306.
4. Couture, L. A., and Stinchcomb, D. T. (1996) *Trends Genet. 12*, 510−515.
5. Jones, J. T., and Sullenger, B. A. (1997) *Nat. Biotechnol. 15*, 902−905.
6. Pley, H. W., Flaherty, K. M., and McKay, D. B. (1994) *Nature 372*, 68−74.
7. Scott, W. G., Finch, J. T., and Klug, A. (1995) *Cell 81*, 991−1002.
8. Hertel, K. J., Herschlag, D., and Uhlenbeck, O. C. (1994) *Biochemistry 33*, 3374−3385.
9. Fedor, M. J., and Uhlenbeck, O. C. (1990) *Proc. Natl. Acad. Sci. U.S.A. 87*, 1668−1672.
10. Freier, S. M., Kierzek, R., Jaeger, J. A., Sugimoto, N., Caruthers, M. H., Neilson, T., and Turner, D. H. (1986) *Proc. Natl. Acad. Sci. U.S.A. 83*, 9373−9377.
11. Milligan, J. F., and Uhlenbeck, O. C. (1989) *Methods Enzymol. 180*, 51−62.
12. Wincott, F., DiRenzo, A., Shaffer, C., Grimm, S., Tracz, D., Workman, C., Sweedler, D., Gonzalez, C., Scaringe, S., and Usman, N. (1995) *Nucleic Acids Res. 23*, 2677−2684.
13. Fedor, M. J., and Uhlenbeck, O. C. (1992) *Biochemistry 31*, 12042−12054.
14. Werner, M., and Uhlenbeck, O. C. (1995) *Nucleic Acids Res. 23*, 2092−2096.
15. Baiyda, N., and Uhlenbeck, O. C. (1997) *Biochemistry 36*, 1108−1114.
16. Stage-Zimmermann, T. K., and Uhlenbeck, O. C. (1998) *RNA 4*, 875−889.
17. Turner, D. H., Sugimoto, N., and Freier, S. M. (1988) *Annu. Rev. Biophys. Biophys. Chem. 17*, 167−192.
18. Serra, M. J., and Turner, D. H. (1995) *Methods Enzymol. 259*, 242−261.
19. Narlikar, G. J., Khosla, M., Usman, N., and Herschlag, D. (1997) *Biochemistry 36*, 2463−2477.
20. Heus, H. A., and Pardi, A. (1991) *J. Mol. Biol. 217*, 113−124.
21. Pörschke, D., and Eigen, M. (1971) *J. Mol. Biol. 62*, 361−381.
22. Ravetch, J., Gralla, J., and Crothers, D. M. (1974) *Nucleic Acids Res. 1*, 109−127.
23. Breslauer, K. J., and Bina-Stein, M. (1977) *Biophys. Chem. 7*, 211−216.
24. Hertel, K. J., Herschlag, D., and Uhlenbeck, O. C. (1996) *EMBO J. 15*, 3751−3757.
25. Herschlag, D. (1995) *J. Biol. Chem. 270*, 20871−20874.
26. Uhlenbeck, O. C. (1995) *RNA 1*, 4−6.
27. de Smit, M. H., and van Duin, J. (1994) *J. Mol. Biol. 235*, 173−184.
28. de Smit, M. H., and van Duin, J. (1994) *J. Mol. Biol. 244*, 144−150.
29. Hertel, K. J., Peracchi, A., Uhlenbeck, O. C., and Herschlag, D. (1997) *Proc. Nat. Acad. Sci. U.S.A. 94*, 8497−8502.
30. Hertel, K. J., Pardi, A., Uhlenbeck, O. C., Koizumi, M., Ohtsuka, E., Uesugi, S., Cedergren, R., Eckstein, F., Gerlach, W. L., Hodgson, R., and Symons, R. H. (1992) *Nucleic Acids Res. 20*, 3252.

BI981740B